We are IntechOpen,
the world's leading publisher of Open Access books
Built by scientists, for scientists

6,900
Open access books available

186,000
International authors and editors

200M
Downloads

Our authors are among the

154
Countries delivered to

TOP 1%
most cited scientists

12.2%
Contributors from top 500 universities

WEB OF SCIENCE™

Selection of our books indexed in the Book Citation Index
in Web of Science™ Core Collection (BKCI)

Interested in publishing with us?
Contact book.department@intechopen.com

Aluminum Mineral Processing and Metallurgy: Iron-Rich Bauxite and Bayer Red Muds

Yingyi Zhang, Yuanhong Qi and Jiaxin Li

Abstract

Bauxite is the main source for alumina production. With the rapid development of iron and steel industry and aluminum industry, high-quality iron ore and bauxite resources become increasingly tense. However, a lot of iron-rich bauxite and Bayer red mud resources have not been timely and effectively recycled, resulting in serious problems of environmental pollution and wastage of resources. The comprehensive utilization of iron-rich bauxite and red mud is still a worldwide problem. The industrial stockpiling is not a fundamental way to solve the problems of iron-rich bauxite and red mud. As to the recovery of valuable metals from iron-rich bauxite and red mud, there are a lot of technical and cost problems, which are serious impediments to industrial development. Applying red mud as construction materials like cement, soil ameliorant applications face the problem of Na, Cr, As leaching into the environment. However, the high-temperature reduction, smelting and alkaline leaching process is a feasible method to recover iron and alumina from iron-rich bauxite and red mud. This chapter intends to provide the reader an overview on comprehensive utilization technology of the low-grade iron-rich bauxite and Bayer red mud sources.

Keywords: bauxite, iron-rich bauxite, Bayer red mud, Bayer process, magnetic separation, reduction and smelting process

1. Introduction

With 8.30%, aluminum is the third element in the earth's crust after the oxygen and the silicon, and for that reason, aluminum minerals are abundant with more than 250 kinds. They are mainly composed of bauxite, kaolinite and alunite. However, only the bauxite is used as source for alumina (Al_2O_3) production. As of 2017, approximately 95% of the world's bauxite production is processed first into alumina, and then into aluminum by electrolysis [1]. The bulk of bauxite production is used as feed for the manufacture of alumina via a wet chemical caustic leach process known as the Bayer process [2]. The majority of the alumina produced from this refining process is smelted using the Hall-Héroult process to produce aluminum metal by electrolytic reduction in a molten bath of natural or synthetic cryolite ($NaAlF_6$) [3]. With the rapid development of iron and steel industry and aluminum industry, high-quality iron ore and bauxite resources become increasingly tense. However, a lot of iron-rich bauxite and Bayer red mud resources have not been

timely and effectively recycled, resulting in serious problems of environmental pollution and resources waste. The comprehensive utilization of low-grade iron-rich bauxite and secondary aluminum mineral sources has attracted worldwide attention. It is an effective way to improve the efficient utilization of resources and the added value of products by using the scientific metallurgical recycling methods. This chapter intends to provide the reader with an overview on comprehensive utilization technology of the low grade iron-rich bauxite and secondary aluminum mineral sources.

2. Bayer process alumina production

Bauxite ore is the main raw material used in alumina production. The alumina production in major regions of the world in 2017 is shown in **Figure 1**. It can be seen that the growth in aluminum production continues to be driven by countries in Asia and the Gulf area, 2017 global aluminum production is nearly 126 million tons, and China has contributed with about 56% (70.7 million tons).

Though alumina can be produced from bauxite under alkaline conditions using lime sinter process and sodium carbonate (Deville Pechiney process) at high temperature in reducing environment with presence of coke and nitrogen [4], the alkalinization by the use of sodium hydroxide (Bayer process) is the most economical process which is employed for purification of bauxite if it contains considerable amount of Fe_2O_3 [5]. Almost 90% of world's alumina production is from bauxite by the Bayer process. The bauxite ore with high alumina content and a high mass ratio of alumina to silica (A/S ratio) is preferred in the alumina industry. The free silica leads to the formation of Bayer sodalite with important losses of sodium hydroxide and alumina in the muds (near to 30%) [6].

The production process of Bayer alumina is shown in **Figure 2**. In the Bayer process, bauxite is leached with a hot solution of sodium hydroxide (NaOH) at temperature of 150–240°C and at 1–6 atm pressure [7]. The aluminum minerals in the bauxite may be present as gibbsite ($Al(OH)_3$), boehmite (AlOOH) or diaspore (AlOOH) [8]. The different forms of the aluminum component will dictate the

Figure 1.
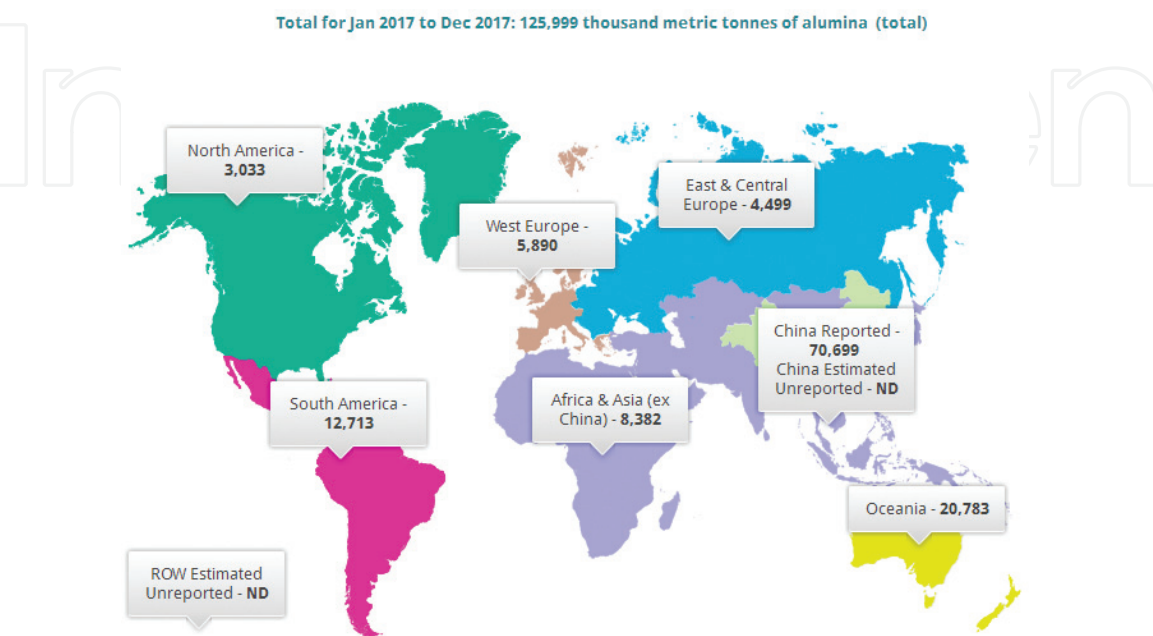*Alumina production in major regions of the world in 2017.*
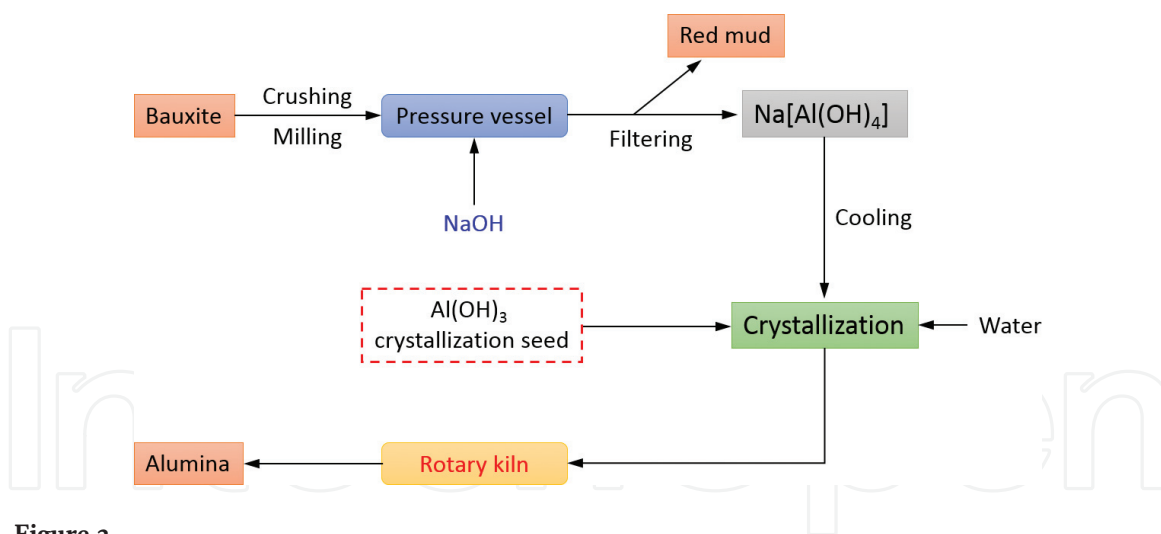
Figure 2.
The process flowsheet of Bayer alumina production.

extraction conditions. The undissolved waste and bauxite tailings contain iron oxides, silica, calcia, titania and some unreacted alumina. After separation of the residue by filtering, pure gibbsite (also known as bayerite) is precipitated when the liquid is cooled, and then seeded with fine-grained aluminum hydroxide. The gibbsite is usually converted into aluminum oxide, and then the aluminum hydroxide decomposes to alumina (Al_2O_3) by heating in rotary kilns or fluid flash calciners at a temperature in excess of 1000°C [9]. This aluminum oxide is dissolved at a temperature of about 960°C in molten cryolite. Next, this molten substance is smelted into the metallic aluminum by the process of electrolysis, which is called the Hall-Héroult process, named in Ref. to the American and French inventors of the process [10].

3. Iron-rich bauxite processing and metallurgy

Iron-rich bauxite ore usually contains over 40 wt% iron oxide [11, 12], huge reserves are found in Australia, Guinea, Brazil, Laos, Vietnam and China, but they have not yet been used effectively. It is worth noting that more than 1.5 billion tons of iron-rich bauxite resources have been explored over the last 20 years in western Guangxi, China [13–15], which belong to the high-iron, low-aluminum silicon ratio type bauxite. These bauxites are very difficult to be leached by the Bayer process also and cannot be used as blast furnace burden. Iron-rich bauxite contains large amounts of silica and iron oxide with complex mineralogical composition and characteristics, which limit the use of this material as feedstock for conventional processes.

China's bauxite reserves are only 3% of the world's bauxite reserves, mainly deposited in Shanxi, Guizhou, Henan and Guangxi provinces. However, the iron-rich bauxite accounts for more than 30% of China's total bauxite resources, which has a great deal of economic value, and more than 1.5 billion tons have been explored in the last 20 years. The typical iron-rich bauxite deposited in Guigang of Guangxi, China is shown in **Figure 3**.

3.1 Mineralogical characteristics of iron-rich bauxite

The typical iron-rich bauxite ore was provided by the Guigang Mine of Guangxi, China. The chemical composition of the iron-rich bauxite is shown in **Table 1**. It can be seen that the iron-rich bauxite mainly consisted of 40.42 wt% Fe_2O_3, 11.70 wt%
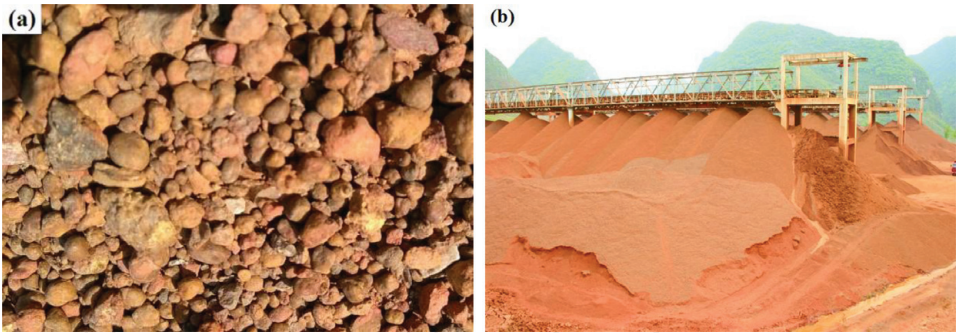
Figure 3.
The typical iron-rich bauxite ore (a) and mineral powder (b) deposited in Guigang of Guangxi, China.

Fe$_{tot}$	Fe$_2$O$_3$	FeO	SiO$_2$	Al$_2$O$_3$	TiO$_2$	MnO	MgO	CaO	LOI
28.29	40.42	0.20	11.77	26.53	1.57	1.21	0.48	1.38	16.42

Table 1.
Chemical composition of iron-rich bauxite sample.

SiO$_2$, and 26.53 wt% Al$_2$O$_3$. The particle size distribution of iron-rich bauxite is shown in **Figure 4(a)** which was obtained with the Malvern Mastersizer 2000 particle size analyzer. The analysis results show that the average particle diameter and specific surface area of mixtures are 88.431 μm and 0.149 m^2/g, respectively. The mineral phase composition of iron-rich bauxite was identified by X-ray diffraction (XRD) as shown in **Figure 4(b)**. It can be seen that the gibbsite [Al(OH)$_3$], diaspore [AlO(OH)], goethite [FeO(OH)], hematite (Fe$_2$O$_3$) and kaolin (Mg$_2$Si$_3$O$_8$·2H$_2$O) are major mineral components in bauxite ore, the anatase (TiO$_2$) and quartz (SiO$_2$) are minor components.

The ore microscope observation shows that the mineral components in the bauxite ores are cryptocrystalline diaspore, hematite, ferrihydrite, kaolinite, anatase, vanadium titanomagnetite and chamosite (**Figure 5(a)**–**(f)**). It can be seen that most of the diaspores are cryptocrystalline with a small particle size and mainly coexists with ferrihydrite (**Figure 5(d) and (f)**). Kaolinite is the major clay mineral in the iron-rich bauxite. Kaolinite mainly coexists with gibbsite and anatase, and the edges of the gibbsite that are adjacent to the kaolinite show clear corrosion (**Figure 5(b)**), suggesting that kaolinite may have formed partially at the expense of gibbsite. Although most of the gibbsite are lamellar (**Figure 5(a)**), small amounts of euhedral-hypidiomorphic gibbsite (50–300 μm) could be discovered in the matrix of the bauxite ores (**Figure 5(b)**). Most of the gibbsite in nature was transformed
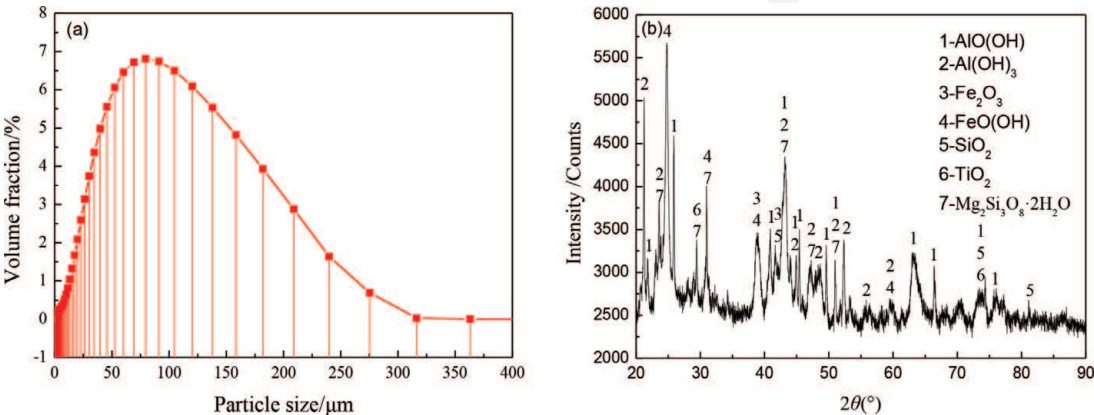

Figure 4.
The particle size distribution (a) and XRD pattern (b) of typical iron-rich bauxite sample.
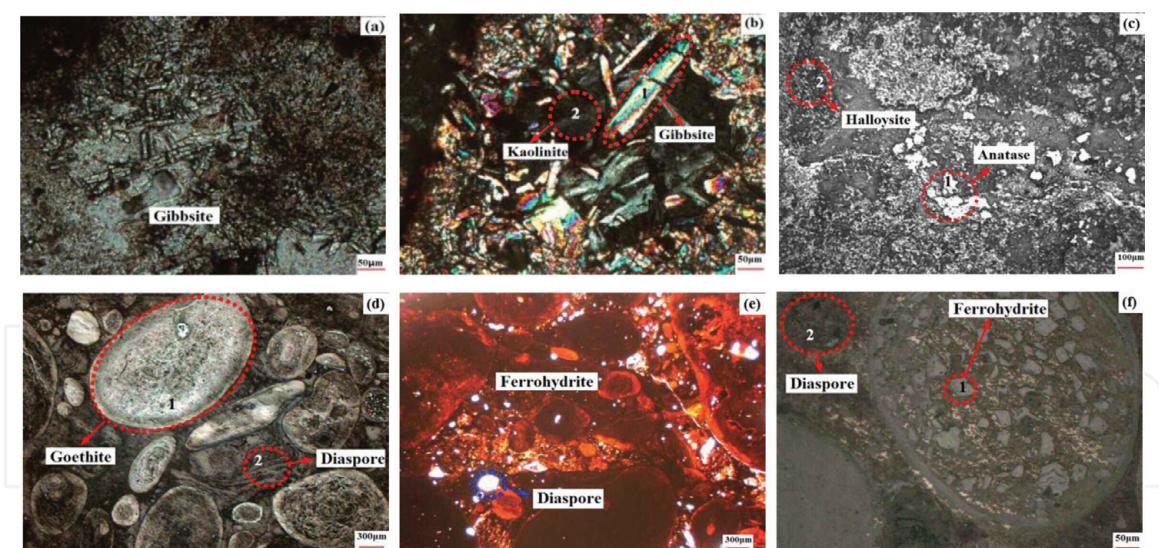
Figure 5.
The microphotographs of typical iron-rich bauxite sample.

from K-feldspar and clay minerals during laterization processes, and it is character-ized by a small crystal size. The gibbsite with relatively perfect crystals was com-monly formed via precipitation from Al-rich solutions within the bauxite horizon. Anatase commonly precipitated in a reducing condition in the formation of the karst bauxite deposit [16, 17].

3.2 Comprehensive utilization processes of iron-rich bauxite

The heterogeneous minerals in iron-rich bauxite are treated with conventional techniques, such as gravity concentration [18], magnetic separation [19], flotation [20], roasting followed by magnetic separation [21, 22] and chemical leaching [23, 24]. All of these conventional techniques cannot recover iron and aluminum from iron-rich bauxite effectively. The reverse flotation process of iron-rich bauxite cannot achieve effective separation of Al_2O_3 and SiO_2, because it is characterized by a high content of Al_2O_3 and SiO_2 and a low ratio of Al_2O_3 to SiO_2 ($m(Al_2O_3)/m$ (SiO_2) = A/S, usually 2–3) [25]. In order to produce a raw material suitable for sponge, the microwave reduction roasting and wet magnetic separation process of red mud was reported, only the total iron concentration of 35.15 and metallization degree of 69.3 wt% were obtained in the process [21]. The lateritic bauxite hydrochloric acid leaching process showed that when the ore granularity was less than 55 μm, the liquid/solid ratio (L/S ratio) was 100:7, the leaching temperature was 373–383 K, the leaching time was 120 min and the HCl concentration was 10%, both the leaching rates of Al and Fe were over 95% [26]. But the hydrochloric acid leaching process was very expensive and caused serious environment pollution.

However, the high-temperature reduction and smelting process exhibit a lot of advantages for ironmaking [27, 28]. In this processes, carbon composite pellets are reduced and smelted to produce metallic iron, which is then separated from slag at a furnace temperature of 1573 K or higher. High-quality iron nuggets are an ideal feed material for steelmaking and can be used for electric arc furnace charging or as a basic oxygen furnace coolant [29, 30]. Zhang et al. [31] successfully obtained iron nuggets and autogenously pulverizable calcium aluminate slag from iron-rich bauxite through a high-temperature reduction and smelting process. The flow dia-gram for recovering iron and autogenously pulverizable slag from iron-rich bauxite is shown in **Figure 6**.
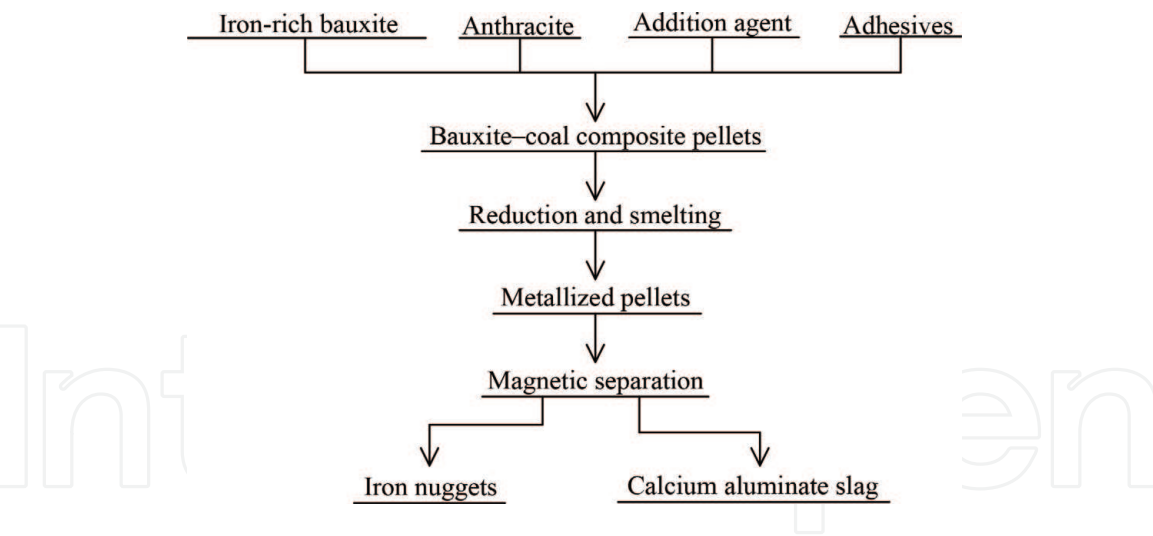
Figure 6.
The flow diagram for recovering iron and autogenously pulverizable slag from high-ferrous bauxite.
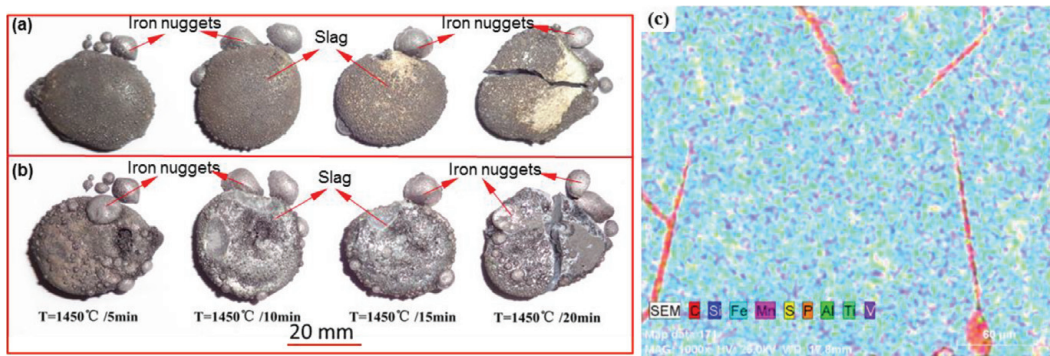

Figure 7.
The photos of iron nuggets and calcium aluminate slag obtained under the optimized process conditions. (a) metallized pellets surfaces, (b) metallized pellets bottoms, (c) EDS map of an iron nugget.

Chemical composition of the iron nuggets/wt%						
Fe	C	Si	S	P	Mn	
93.28	4.17	0.12	0.0043	0.0064	1.60	
Chemical composition of the autogenously pulverizable slag/wt%						
FeO	Al_2O_3	SiO_2	CaO	MnO	TiO_2	MgO
1.28	27.21	13.69	52.83	1.35	1.74	0.85

Table 2.
Chemical composition of the iron nuggets and autogenously pulverizable slag.

They found that the optimized process conditions were bauxite/anthracite/ slaked lime weight ratio of 100:16.17:59.37, reduction temperature at 1450°C and reduction time of 20 min. Under these conditions, high-quality iron nuggets and calcium aluminate slag were obtained and shown in **Figure 7**. The largest size and the highest recovery rate of iron nuggets were 11.42 mm and 92.79 wt%, respectively. The chemical composition of the iron nuggets and autogenously pulverizable calcium aluminate slag is shown in **Table 2**. It can be seen that the iron nuggets mainly consist of Fe, C and Mn. The total iron content exceeds 93.28 wt%, and the C and Mn contents are 4.17 and 1.60 wt%, respectively. Almost no harmful elements are present, specifically S and P. The chemical composition of autogenously pulverizable slag mainly consisted of Al_2O_3 (27.21 wt%), SiO_2 (13.69 wt%) and CaO

Figure 8.
The cement clinker of autogenously pulverizable slag. (a) R = 3.60, (b) R = 3.85, (c) R = 4.10.

(52.83 wt%), and the mineral constituent mainly comprised Ca_2SiO_4 and $Ca_{12}Al_{14}O_{33}$, with small amounts of $FeAl_2O_4$, $CaAl_2O_4$ and $Ca_2Al_2SiO_7$.

In addition, Zhang et al. [32] found that the autogenously pulverizable slag (calcium aluminate slag) cement clinker has a higher reactivity during the early stage of the hydration process, and the cement clinker of autogenously pulverizable slag is shown in **Figure 8**. After hydration for 28 days, the hydration products of autogenously pulverizable slag are mainly composed of killalaite ($Ca_{3.2}(H_{0.6}Si_2O_7)$ (OH)), calcium silicate hydrate ($Ca_{1.5}SiO_{3.5}\cdot xH_2O$) and calcium aluminates hydroxide ($3CaO\cdot Al_2O_3\cdot Ca(OH)_2\cdot 18\cdot H_2O$, $Ca12Al_{13.86}Fe_{0.14}(OH)_2$). With the increase of w $(CaO)/w(SiO_2)$ ratios, the killalaite disappeared, the $3CaO\cdot Al_2O_3\cdot Ca(OH)_{2.18}\cdot H_2O$ and $Ca_{12}Al_{13.86}Fe_{0.14}(OH)_2$ amounts increases gradually as a function of w(CaO)/w (SiO_2) ratio. The C_3A and $C_{12}A_7$ have very exothermic hydration characteristic and faster hydration rate, promoted the hydration activity of β-C_2S.

The autogenously pulverizable slag (calcium aluminate slag) can also be applied to leach alumina with Na_2CO_3 and Na_2C solutions [33, 34]. The ideal composition of calcium aluminate slags is $12CaO\cdot 7Al_2O_3$ and γ-$2CaO\cdot SiO_2$ [35]. The slag reacts with sodium carbonate solution and yields an alumina leaching efficiency of 85% [36]. Therefore, the high-temperature reduction, smelting and alkaline leaching process is a feasible method to recover iron and alumina from iron-rich bauxite.

4. Iron-rich red mud processing and metallurgy

Red mud is the solid waste residue generated from the alumina refining of bauxite ore, primarily by the Bayer process which utilizes caustic soda to dissolve the aluminum silicate. Approximately, 35–40% of the processed bauxite ore goes into the waste as alkaline red mud slurry which consists of 15–40% solids, and 1.0–1.5 tons of red mud is generated per ton of alumina produced [37]. It is estimated that annually 70 million tons of red mud is produced all over the world, with 0.7 million tons in Greece, 2 million tons in India, 30 million tons in Australia, nearly 30 million tons in China [38, 39] and presently it has been already accumulated in well over 4.0 billion tons [40]. With the quick development of alumina industry, the disposal of red mud has caused serious environmental problems mainly due to its large quantities and strong alkalinity (pH 10.0–12.5) [41]. At present, only little red mud is used to produce construction materials and calcination cement [42, 43]. Most of the red mud is directly placed in landfill, deep sea and storage in settling ponds, as shown in **Figure 9**. Despite the harmful impact that these methods pose on our environment, the risks of failure of a poorly engineered storage dam can result in even greater social and economic damage.
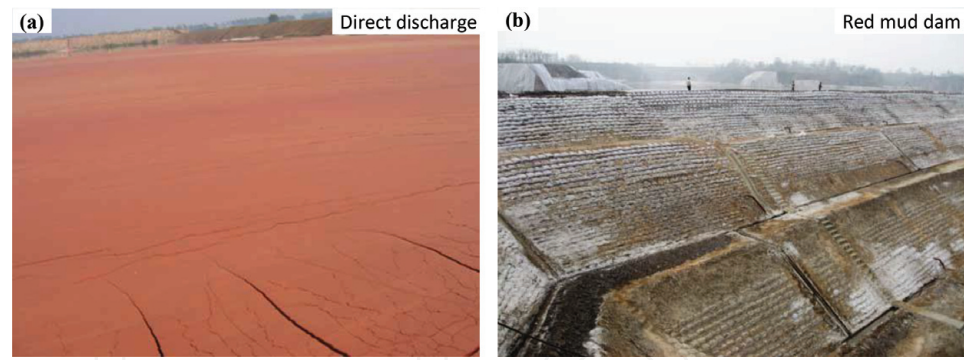
Figure 9.
The traditional disposal method of red mud.

Chemical composition	Concentration (wt%)	Major elements	Concentration (wt%)	Minor elements	Concentration (mg/kg)
Fe_2O_3	30–65	Fe	4.52–50.6	U	50–60
Al_2O_3	10–20	Al	4.42–16.06	Ga	60–90
SiO_2	3–30	Si	2.16–14.86	V	730
Na_2O	2–10	Na	0.98–7.79	Zr	1230
CaO	2–8	Ca	0.39–16.72	Sc	54–120
TiO_2	Trace-15	Ti	0.98–5.34	Cr	497

Table 3.
Typical chemical composition and metal content of red mud [37, 45, 46].

4.1 Mineralogical characteristics of iron-rich red mud

Red mud is mainly composed of coarse sand and fine particles of mud. Its composition, property and phase vary with the origin of the bauxite and the alumina production process, and will change over time when stocked [44]. No matter what the production process is, the chemical composition of red mud contains six major constituents. Chemical analysis shows that red mud contains Si, Al, Fe, Ca, Ti, Na, as well as an array of minor elements, namely U, Ga, V, Zr, Sc, Cr, Mn, Ni, Zn etc. [37, 45, 46]. The variation in chemical composition between red mud worldwide is very high. Typical chemical composition and metal content of Bayer process red mud are shown in **Table 3**. The calcium oxide (CaO) and silica (SiO_2) are the major constituents for red mud from the sintering process, but the contents of Fe_2O_3 in red mud from the sintering process and combined process are much lower than that from the Bayer process. The major chemical composition of iron-rich red mud generated in alumina plants in various countries over the world is presented in **Table 4**.

Generally, the major mineralogical constituents of iron-rich red mud from the Bayer process are gibbsite ($Al(OH)_3$), boehmite (γ-AlOOH), hematite (Fe_2O_3), goethite (FeO(OH)), quartz (SiO_2), rutile (TiO_2), anatase (TiO_2) and calcite ($CaCO_3$) [47, 48], and the principal mineralogical constituents of red mud from the sintering process are β-2CaO·SiO_2, calcite ($CaCO_3$), aragonite ($CaCO_3$), hematite (Fe_2O_3), gibbsite ($Al(OH)_3$) and perovskite ($CaTiO_3$) [49, 50]. Red mud is a very fine grained material with an average particle size <10 μm. Typical values for particle size distribution are 90 wt% below 75 μm [51]. The specific surface area (BET) of red mud is between 10 and 30 m^2/g, depending on the degree of grinding of bauxite.

Country	Plant	Major composition (wt%)							Ref. No.
		Al_2O_3	Fe_2O_3	SiO_2	TiO_2	CaO	Na_2O	A/S	
Italy	Eurallumina	20.00	35.2	11.6	9.20	6.70	7.50	1.72	[52]
Turkey	Seydisehir	20.39	36.94	15.74	4.98	2.23	10.10	1.30	[53]
UK	ALCAN	20.00	46.00	5.00	6.00	1.00	8.00	4.00	[54]
Canada	ALCAN	20.61	31.60	8.89	6.23	1.66	10.26	2.32	[55]
Australia	Tomakomai	19.78	46.14	10.92	9.79	6.15	7.14	1.81	[56]
	Pinjarra	19.77	41.85	27.51	4.51	4.51	1.85	0.72	[57]
Brazil	Alunorte	15.1	45.60	15.60	4.29	1.16	7.50	0.97	[58]
Germany	AOSG	16.20	44.80	5.40	12.33	5.22	4.00	3.00	[58]
USA	RMC	18.4	35.50	8.50	6.31	7.73	6.10	2.16	[58]
	Point Comfort	20.67	46.44	11.13	9.85	8.79	3.12	1.86	[56]
India	Damanjodi	17.01	62.99	7.36	4.25	2.87	5.52	2.31	[59]
	Belgaum	21.57	50.00	7.87	15.17	0.90	4.49	2.74	[59]
China	Chinalco	19.08	36.13	28.19	0.77	2.84	12.99	0.68	[60]

Table 4.
Major chemical composition of iron-rich red mud generated in alumina plants in various countries.
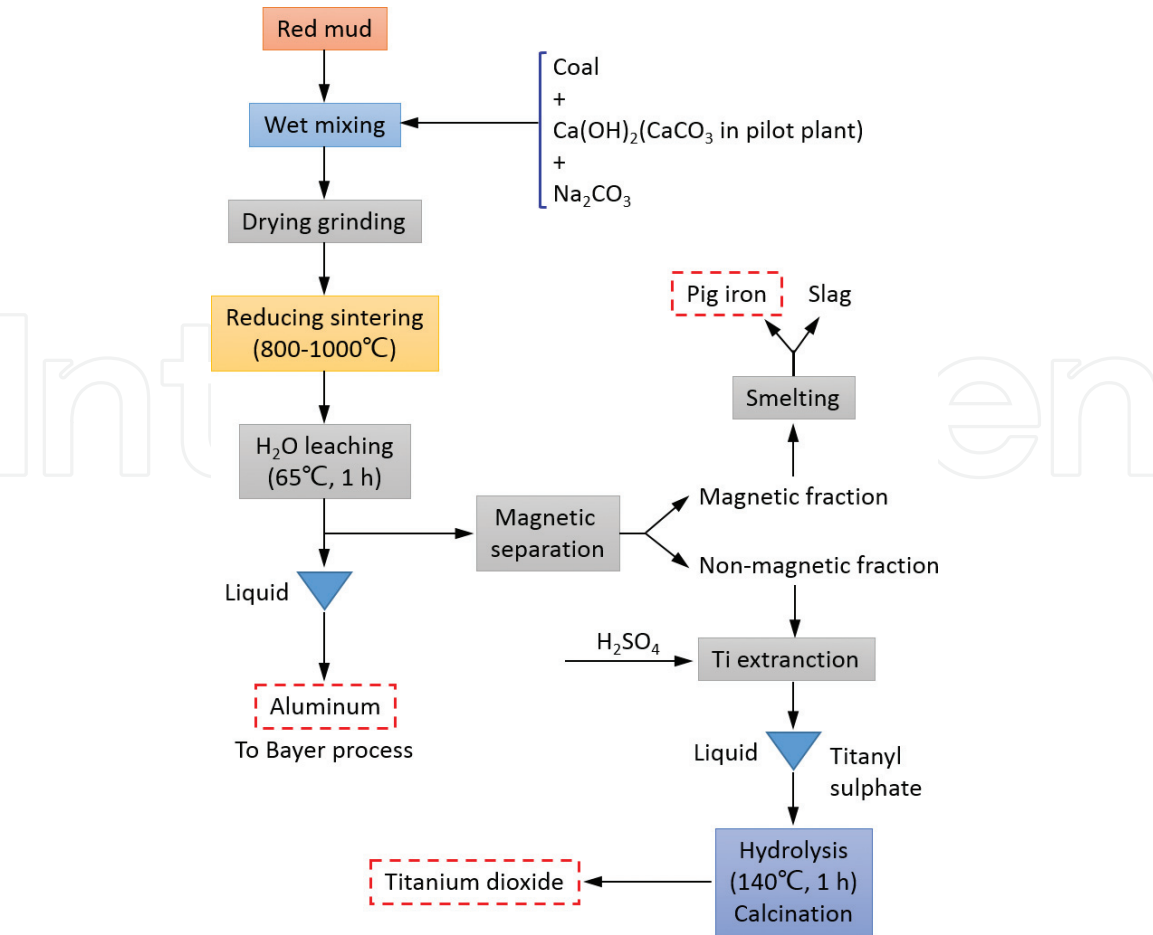

Figure 10.
Process flowsheet for metal extraction from red mud by a combined pyro- and hydrometallurgical process [67].

4.2 Comprehensive utilization processes of iron-rich red mud

During the past decades, extensive work has been done by a lot of researchers to develop various economic ways for the utilization of red mud. Such as the red mud from sintering process, containing some reactive substance such as β-2CaO·SiO$_2$, can be used to produce construction materials directly [49, 61]. However, in Bayer process, Al$_2$O$_3$ is dissolved depending on sodium hydroxide from high-iron, high-aluminum boehmite and gibbsite bauxite without calcination. Thus, there is less pozzolanic active substance in the Bayer red mud. It is not feasible to use red mud from Bayer process as construction materials directly [62]. Tsakiridis et al. [43] reported the research work on Bayer red mud addition in the raw meal for the production of Portland cement clinker. However, only 3–5% red mud can be mixed with other raw materials, and it is not an effective way compared with the huge amount of the produced red mud. Pontikes et al. [63] did some research work on the thermal behavior of clay mixtures with bauxite residue for the production of heavy-clay ceramics, which has potential utilization of red mud in industries. However, this method does not give full play to the potential value of red mud, and the
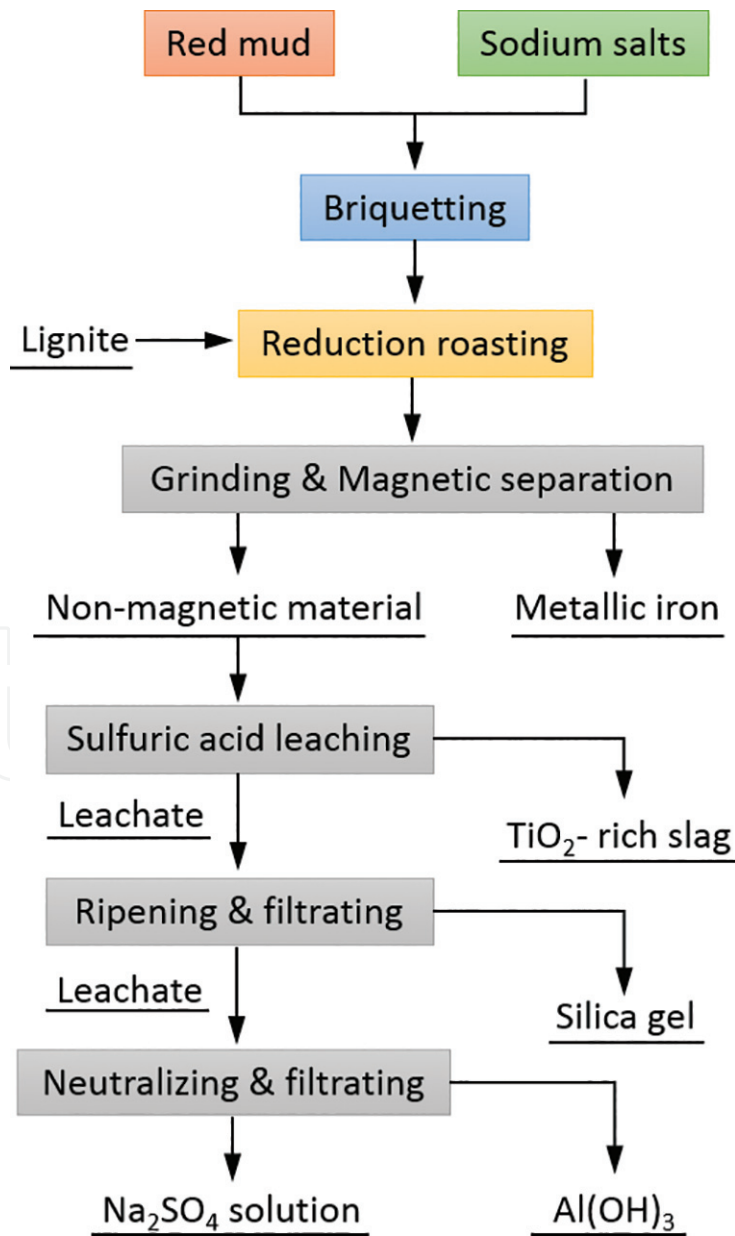

Figure 11.
Process flowsheet for reduction, roasting and magnetic separation process of red mud [68].

valuable metals in red mud are not utilized effectively. Some techniques of recovery of rare elements from red mud are not applied because of the complicated procedure and high cost, although some useful production such as gallium (Ga), titanium dioxide (TiO_2) and scandium (Sc) can be obtained [64–66].

As the high-iron content of the Bayer red mud, there are many techniques that have been intensively investigated for practical implementation with the purpose of recovering valuable components from this waste, such as combined pyrometallurgy and hydrometallurgical process [67], solid-state carbothermic reduction and magnetic separation [68], acid leaching [67] and smelting in a blast furnace [69]. A new concept of using red mud directly for ironmaking/smelting gives further promise.

A combined pyrometallurgical and hydrometallurgical process could also be employed to recover aluminum, iron and titanium elements [67]. The process flowsheet is shown in **Figure 10**. It can be seen that the red mud was first dried and then mixed with coal, lime and sodium carbonate. The mixture is reduced and sintered at 800–1000°C. The sintered products underwent water leaching at 65°C for 1 h and 89% aluminum involved in the products was leached out. The filtrate obtained can be recycled in the Bayer process, and the residue was subjected to high-intensity magnetic separation. The titanium in the non-magnetic portion was taken to the solution by leaching with sulfuric acid. The titanyl sulfate was filtered and then hydrolyzed to metatitanic acid. This acid was then roasted to form TiO_2 (87–89% grade). At last, the magnetic portion was smelted at 1480°C and a product containing 93–94% Fe, 4.5% C, was obtained.

Li et al. [68] carried out stepwise extraction of valuable components like Fe_2O_3, Al_2O_3 and SiO_2 from reduced red mud by magnetic separation and sulfuric acid leaching. During the reductive roasting of red mud, sodium played an important role in reducing the dispersity of iron and hence increased the efficiency of magnetic separation. They found that the red mud was reduced at 1050°C for 60 min in
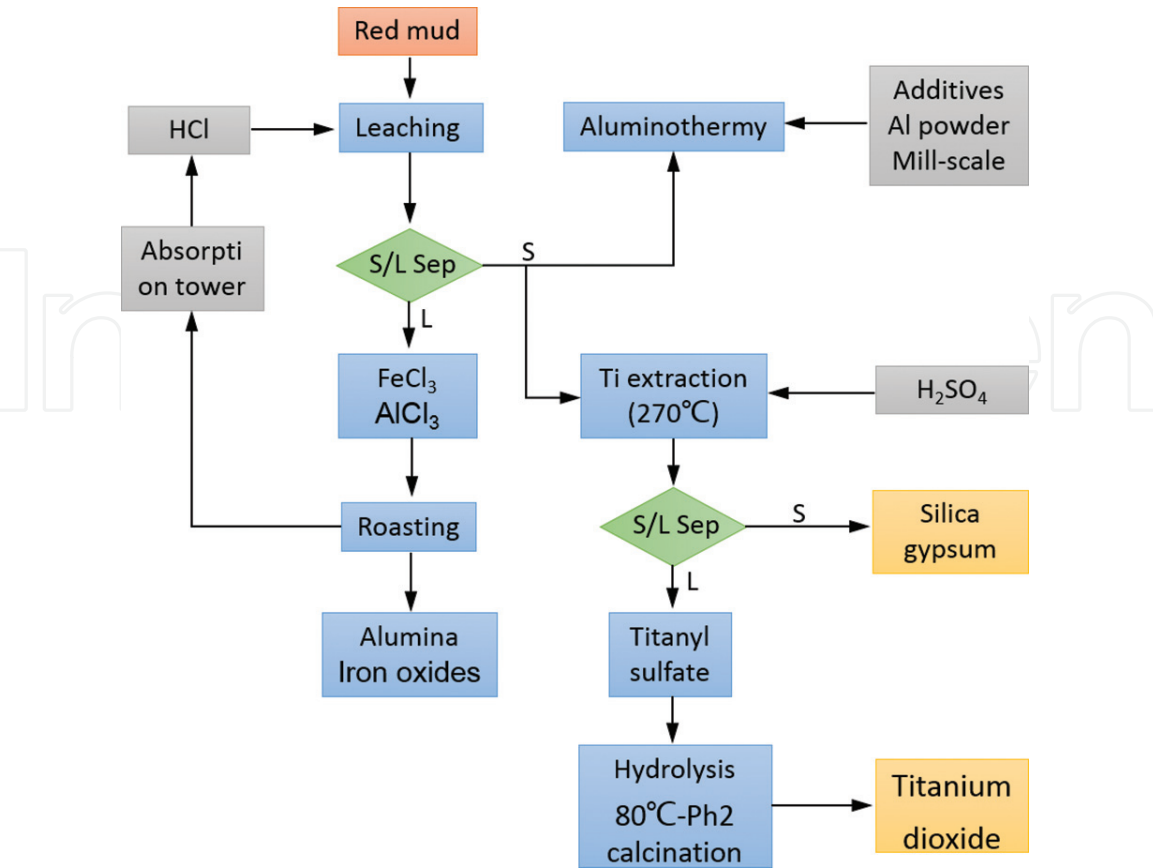

Figure 12.
Process flowsheet for metal recovery from red mud [67].

the presence of 6% Na_2CO_3 and 6% Na_2SO_4. In the enrichment of TiO_2 by sulfuric acid leaching, 94.7% Fe, 98.6% Al and 95.9% Si were extracted and left behind a material having 37.8% TiO_2. The process flowsheet for reduction, roasting and magnetic separation process of red mud is shown in **Figure 11**.

Piga et al. [67] used the acid leaching process to dispose the red mud, and they found that the titanium is soluble in sulfuric acid but not in hydrochloric acid. This process increased the recovery of TiO_2 content in the residue from 31 to 58%. The solids were then leached with sulfuric acid at 270°C, followed by hydrolysis and roasting. The TiO_2 content obtained was 96%. The product can be used directly as TiO_2 pigment or chlorinated to form $TiCl_4$. The process flowsheet for TiO_2 recovery from red mud is shown in **Figure 12**.

5. Conclusions

The comprehensive utilization of iron-rich bauxite and red mud is still a worldwide problem. At current levels of technology and practice, the capacity of consumption and secondary utilization is seriously insufficient. A large number of iron-rich bauxite and red mud have not been used effectively. The industrial stockpiling is not a fundamental way to solve the problems of iron-rich bauxite and red mud. As to the recovery of valuable metals from iron-rich and red mud, there are a lot of technical and cost problems, which cause serious impediments to industrial development. Therefore, we must decrease the recycling process costs and energy consumption, promote the industrialization of valuable metals recovery processes, optimize complex processes and develop new processes. Applying red mud as construction materials like cement, soil ameliorant applications, face the problem of Na, Cr, As leaching into the environment. However, the high-temperature reduction, smelting and alkaline leaching process is a feasible method to recover iron and alumina from iron-rich bauxite and red mud. Due to the simple process, low cost, it is worth promoting its application in the field of iron and steel industry and aluminum industry.

Acknowledgements

Author details

Yingyi Zhang[1,2]*, Yuanhong Qi[3] and Jiaxin Li[1]

1 School of Metallurgical Engineering, Anhui University of Technology, Maanshan, Anhui Province, PR China

2 College of Material Science and Engineering, Chongqing University, Chongqing, PR China

3 State Key Laboratory of Advance Steel Processes and Products, Central Iron and Steel Research Institute, Beijing, PR China

*Address all correspondence to: zhangyingyi@cqu.edu.cn

References

[1] Boni M, Rollinson G, Mondillo N, et al. Quantitative mineralogical characterization of karst bauxite deposits in the southern Apennines, Italy. Economic Geology. 2013;**108**(4): 813-833. DOI: 10.2113/econgeo.108.4.813

[2] Djurić I, Mihajlović I, Živković Ž. Kinetic modelling of different bauxite types in the bayer leaching process. Canadian Metallurgical Quarterly. 2013;**49**(3):209-218. DOI: 10.1179/cmq.2010.49.3.209

[3] Mahadevan H, Ramachandran TR. Recent trends in alumina and aluminium production technology. Bulletin of Materials Science. 1996;**19**(6):905-920. DOI: 10.1007/BF02744627

[4] Yu ZL, Chen YM, Niu YJ, et al. Efficient and sustainable production of alumina by electrolysis of sodium carbonate. Angewandte Chemie. 2011;**50**(49):11719-11723. DOI: 10.1002/ange.201104444

[5] Ostap S. Control of silica in the bayer process used for alumina production. Canadian Metallurgical Quarterly. 2013;**25**(2):101-106. DOI: 10.1179/cmq.1986.25.2.101

[6] Zhang R, Zheng SL, Ma SH, et al. Recovery of alumina and alkali in Bayer red mud by the formation of andradite-grossular hydrogarnet in hydrothermal process. Journal of Hazardous Materials. 2011;**189**(3): 827-835. DOI: 10.1016/j.jhazmat.2011.03.004

[7] Hind AR, Bhargava SK, Grocott SC. The surface chemistry of Bayer process solids: A review. Colloids and Surfaces A: Physicochemical and Engineering Aspects. 1999;**146**(1–3): 359-374. DOI: 10.1016/S0927-7757(98)00798-5

[8] Kloprogge JT, Duong LV, Wood BJ, et al. XPS study of the major minerals in bauxite: Gibbsite, bayerite and (pseudo-) boehmite. Journal of Colloid and Interface Science. 2006;**296**(2):572-576. DOI: 10.1016/j.jcis.2005.09.054

[9] Xie ZP, Lu JW, Huang Y, et al. Influence of α-alumina seed on the morphology of grain growth in alumina ceramics from Bayer aluminum hydroxide. Materials Letters. 2003;**57**(16–17):2501-2508. DOI: 10.1016/S0167-577X(02)01301-0

[10] Solheim A, Rolseth S, Skybakmoen E, et al. Liquidus temperatures for primary crystallization of cryolite in molten salt systems of interest for aluminum electrolysis. Metallurgical and Materials Transactions B. 1996;**27**(5):739-744. DOI: 10.1007/BF02915602

[11] Papassiopi N, Vaxevanidou K, Paspaliaris I. Effectiveness of iron reducing bacteria for the removal of iron from bauxite ores. Minerals Engineering. 2010;**23**(1):25-31. DOI: 10.1016/j.mineng.2009.09.005

[12] Pickles C A, Lu T, Chambers B, et al. A study of reduction and magnetic separation of iron from high iron bauxite ore. Canadian Metallurgical Quarterly 2013;**51**(4):424-433. DOI: 10.1179/1879139512Y.0000000038

[13] Liu XF, Wang QF, Zhang QZ. Mineralogical characteristics of the superlarge quaternary bauxite deposits in jingxi and debao counties, Western Guangxi, China. Journal of Asian Earth Sciences; 2012;**52**(3):53-62. DOI: 10.1016/j.jseaes.2012.02.011

[14] Wang QF, Deng J, Liu XF, et al. Discovery of the REE minerals and its geological significance in the Quyang bauxite deposit, West Guangxi, China.

Journal of Asia Earth Sciences. 2010; **39**(6):701-712. DOI: 10.1016/j. jseaes.2010.05.005

[15] Liu XF, Wang QF, Deng J, et al. Mineralogical and geochemical investigations of the Dajia Salento-type bauxite deposits, western Guangxi, China. Journal of Geochemical Exploration. 2010;**105**:137-152. DOI: 10.1016/j.gexplo.2010.04.012

[16] Özlü N. Trace element contents of karst bauxites and their parent rocks in the Mediterranean belt. Mineralium Deposita. 1983;**18**:469-476. DOI: 10.1007/BF00204491

[17] Zarasvandi A, Charchi A, Carranza E J M, Alizadeh B. Karst bauxite deposits in the Zagros Mountain belt, Iran. Ore Geology Reviews 2008;**34**:521-532. DOI: 10.1016/j.oregeorev.2008.05.005

[18] Smith P. The processing of high silica bauxites–review of existing and potential processes. Hydrometallurgy. 2009;**98**(1–2):162-176. DOI: 10.1016/j. hydromet.2009.04.015

[19] Bolsaitis P, Chang V, Schorin H, Aranguren R. Beneficiation of ferruginous bauxites by high-gradient magnetic separation. International Journal of Mineral Processing. 1981; **8**(3):249-263. DOI: 10.1016/0301-7516 (81)90015-6

[20] Massola CP, Chaves AP, Lima JRB, Andrade CF. Separation of silica from bauxite via froth flotation. Minerals Engineering. 2009;**22**:315-318. DOI: 10.1016/j.mineng.2008.09.001

[21] Michail S, Maria T, Petros ET, Konstantinos P. Greek "red mud" residue: A study of microwave reductive roasting followed by magnetic separation for a metallic iron recovery process. Journal of Hazardous Materials. 2013;**254-255**:193-205. DOI: 10.1016/j. jhazmat.2013.03.059

[22] Liu YY, Zhao BC, Tang Y, Wan PY. Recycling of iron from red mud by magnetic separation after co-roasting with pyrite. Thermochimica Acta. 2014; **588**:11-15. DOI: 10.1016/j. tca.2014.04.027

[23] Zhao AC, Liu Y, Zhang TA, et al. Thermodynamics study on leaching process of gibbsite bauxite by hydrochloric acid. Transactions of Nonferrous Metals Society of China. 2013;**23**(1):266-270. DOI: 10.1016/ S1003-6326(13)62455-3

[24] Sancho JP, Ayala J, García MP, Fernández B. Leaching behavior of a bayer electro filter fines in sulphuric acid. Hydrometallurgy. 2009;(96): 35-41. DOI: 10.1016/j.hydromet. 2008.07.007

[25] Wang Y, Hu Y, He P, Gu G. Reverse flotation for removal of silicates from diasporic-bauxite. Minerals Engineering. 2004;**17**(1):63-68. DOI: 10.1016/j.mineng.2003.09.010

[26] Zhao AC, Liu Y, Zhang TA, Lv GZ, Dou ZH. Thermodynamics study on leaching process of gibbsitic bauxite by hydrochloric acid. Transactions of Nonferrous Metals Society of China. 2013;**23**(1):266-270. DOI: 10.1016/ S1003-6326(13)62455-3

[27] Zhai XJ, Li NJ, Zhang X, Fu Y, Jiang L. Recovery of cobalt from converter slag of chambishi copper smelter using reduction smelting process. Transactions of Nonferrous Metals Society of China. 2011;**21**(9):2117-2121. DOI: 10.1016/S1003-6326(11)60982-5

[28] Kapure GU, Rao CB, Tathavadkar VD, Sen R. Direct reduction of low grade chromite overburden for recovery of metals. Ironmaking & Steelmaking. 2011;**38**(38):590-596. DOI: 10.1179/ 1743281211Y.0000000028

[29] Ding YG, Wang JS, Wang G, Ma S, Xue QG. Comprehensive utilization of

Paigeite ore using iron nugget making process. Journal of Iron and Steel Research, International. 2012;**19**(6): 9-13. DOI: 10.1016/S1006-706X(12) 60119-8

[30] Guo YH, Gao JJ, Xu HJ, Zhao K, Shi XF. Nuggets production by direct reduction of high iron red mud. Journal of Iron and Steel Research, International. 2013;**20**(5):24-27. DOI: 10.1016/S1006-706X(13)60092-8

[31] Zhang YY, Wei L, Qi YH, et al. Recovery of iron and calcium aluminate slag from high-ferrous bauxite by high-temperature reduction and smelting process. International Journal of Minerals, Metallurgy, and Materials. 2016;**23**(8):881-890. DOI: 10.1007/s12613-016-1303-3

[32] Zhang YY, Qi YH, Zou ZS. Early stage hydration properties of calcium aluminosilicate slag. International Conference on Advanced Design and Manufacturing Engineering (ICADME 2016); 23–24 July 2016; Shenzhen. 2016. pp. 32-38

[33] Yu HY, Pan XL, Ding TT, Zhang W, Liu H, Bi SW. Adsorption of sodium polyacrylate at interface of dicalcium silicate–sodium aluminate solution. Transactions of Nonferrous Metals Society of China. 2011;**21**(10): 2323-2326. DOI: 10.1016/S1003-6326 (11)61015-7

[34] Wang B, Sun HL, Guo D, Zhang XZ. Effect of Na_2O on alumina leaching property and phase transformation of MgO containing calcium aluminate slags. Transactions of Nonferrous Metals Society of China. 2011;**21**(12): 2752-2757. DOI: 10.1016/S1003-6326 (11)61119-9

[35] Yu HY, Pan XL, Wang B, Zhang W, Sun HL, Bi SW. Effect of Na_2O on formation of calcium aluminates in CaO-Al_2O_3-SiO_2 system. Transactions of Nonferrous Metals Society of China.

2012;**22**(12):3108-3112. DOI: 10.1016/S1003-6326(11)61578-1

[36] Bi SW, Yang YH, Li YT, Zhang JD, Duan ZY. Study of alumina leaching from calcium aluminate slag. Light Metals. 1996:10-15

[37] Zhang R, Zheng S, Ma S, et al. Recovery of alumina and alkali in Bayer red mud by the formation of andradite-grossular hydrogarnet in hydrothermal process. Journal of Hazardous Materials. 2011;**189**(3):827-835. DOI: 10.1016/j. jhazmat.2011.03.004

[38] Agrawal A, Sahu KK, Pandey BD. Solid waste management in non-ferrous industries in India. Resources, Conservation and Recycling. 2004; **42**(2):99-120. DOI: 10.1016/j. resconrec.2003.10.004

[39] Wang S, Ang HM, Tadé MO. Novel applications of red mud as coagulant, adsorbent and catalyst for environmentally benign processes. Chemosphere. 2008;**72**(11):1621-1623. DOI: 10.1016/j.chemosphere.2008.05.013

[40] Liu Y, Naidu R. Hidden values in bauxite residue (red mud): Recovery of metals. Waste Management. 2014; **34**(12):2662-2673. DOI: 10.1016/j. wasman.2014.09.003

[41] Liu X, Zhang N, Yao Y, et al. Micro-structural characterization of the hydration products of bauxite-calcination-method red mud-coal gangue based cementitious materials. Journal of Hazardous Materials. 2013; **262**(8):428. DOI: 10.1016/j. jhazmat.2013.08.078

[42] Yang JK, Fan C, Hou J, et al. Engineering application of basic level materials of red mud high level pavement. China Municipal Engineering. 2006

[43] Tsakiridis PE, Agatzini-Leonardou S, Oustadakis P. Red mud addition in

the raw meal for the production of Portland cement clinker. Journal of Hazardous Materials. 2004;**116**(1–2): 103-110. DOI: 10.1016/j. jhazmat.2004.08.002

[44] Liu DY, Wu CS. Stockpiling and comprehensive utilization of red mud research progress. Materials. 2012;**5**(7): 1232-1246. DOI: 10.3390/ma5071232

[45] Sutar H. Progress of red mud utilization: An overview. American Chemical Science Journal. 2014;**4**(3): 255-279. DOI: 10.9734/ACSJ/2014/7258

[46] Wang W, Pranolo Y, Chu YC. Recovery of scandium from synthetic red mud leach solutions by solvent extraction with D2EHPA. Separation and Purification Technology. 2013; **108**(16):96-102. DOI: 10.1016/j. seppur.2013.02.001

[47] Nan XL, Zhang TA, Liu Y, et al. Analysis of comprehensive utilization of red mud in China. The Chinese Journal of Process Engineering. 2010;**10**: 264-270

[48] Nenadović SS, Mucsi G, Kljajević LM, et al. Physicochemical, mineralogical and radiological properties of red mud samples as secondary raw materials. Nuclear Technology and radiation Protection. 2017;**32**(3):261-266. DOI: 10.2298/ NTRP1703261N

[49] Yang J, Xiao B. Development of unsintered construction materials from red mud wastes produced in the sintering alumina process. Construction and Building Materials. 2008;**22**(12): 2299-2307. DOI: 10.1016/j. conbuildmat.2007.10.005

[50] Ying Z, Wang J, Liu CJ, et al. Characterization and risk assessment of red mud derived from the sintering alumina process. Fresenius Environmental Bulletin. 2009;**18**(6): 989-993

[51] Tian Y, Wang FX, Ma SC. The mechanical properties of red mud stockpiling. Light Metals. 1998;**2**:32-34

[52] Sglavo VM, Campostrini R, Maurina S, et al. Bauxite 'red mud' in the ceramic industry. Part 1: Thermal behaviour. Journal of the European Ceramic Society. 2000;**20**(3):235-244. DOI: 10.1016/S0955-2219(99)00088-6

[53] Soner Altundoğan H, Altundoğan S, Tümen F, et al. Arsenic adsorption from aqueous solutions by activated red mud. Waste Management. 2002;**22**(3): 357-363. DOI: 10.1016/S0956-053X(01) 00041-1

[54] Srikanth S, Ray AK, Bandopadhyay A, et al. Phase constitution during sintering of red mud and red mud–fly ash mixtures. Journal of the American Ceramic Society. 2005;**88**(9):2396-2401. DOI: 10.1111/j.1551-2916.2005.00471.x

[55] Vachon P, Tyagi RD, Auclair JC, et al. Chemical and biological leaching of aluminum from red mud. Environmental Science & Technology. 1994;**28**(1):26. DOI: 10.1021/ es00050a005

[56] Hamdy MK, Williams FS. Bacterial amelioration of bauxite residue waste of industrial alumina plants. Journal of Industrial Microbiology & Biotechnology. 2001;**27**(4):228-233. DOI: 10.1038/sj/jim/7000181

[57] Zhang Y, Xu HJ, Cheng XL, et al. Comprehensive utilization of high-iron bauxite and high-iron red mud. Mining Research & Development. 2015;**6**:30-35

[58] Snars K, Gilkes RJ. Evaluation of bauxite residues (red muds) of different origins for environmental applications. Applied Clay Science. 2009;**46**(1):13-20. DOI: 10.1016/j.clay.2009.06.014

[59] Prasad P, Subramanian S. Problems and prospects of red mud utilization.

Transactions of the Indian Institute of Metals. 1997;**50**(5):427-442

[60] Liu W, Yang J, Xiao B. Review on treatment and utilization of bauxite residues in China. International Journal of Mineral Processing. 2009;**93**(3–4):220-231. DOI: 10.1016/j.minpro.2009.08.005

[61] Mymrin VA, Vázquez-Vaamonde AJ. Red mud of aluminium production waste as basic component of new construction materials. Waste Management & Research the Journal of the International Solid Wastes & Public Cleansing Association Iswa. 2001;**19**(5):465-469. DOI: 10.1177/0734242X0101900512

[62] Liu W, Yang J, Bo X. Application of Bayer red mud for iron recovery and building material production from alumosilicate residues. Journal of Hazardous Materials. 2009;**161**(1):474-478. DOI: 10.1016/j.jhazmat.2008.03.122

[63] Pontikes Y, Nikolopoulos P, Angelopoulos GN. Thermal behaviour of clay mixtures with bauxite residue for the production of heavy-clay ceramics. Journal of the European Ceramic Society. 2007;**27**(2–3):1645-1649. DOI: 10.1016/j.jeurceramsoc.2006.05.067

[64] Smirnov DI, Molchanova TV. The investigation of sulphuric acid sorption recovery of scandium and uranium from the red mud of alumina production. Hydrometallurgy. 1997;**45**(3):249-259. DOI: 10.1016/S0304-386X(96)00070-9

[65] Lu F, Xiao T, Lin J, et al. Recovery of gallium from Bayer red mud through acidic-leaching-ion-exchange process under normal atmospheric pressure. Hydrometallurgy. 2017;**175**:124-132. DOI: 10.1016/j.hydromet.2017.10.032

[66] Liu Z, Li H, Jing Q, et al. Recovery of scandium from leachate of Sulfation-roasted Bayer red mud by liquid–liquid extraction. Journal of Metals. 2017;**69**(7):1-6. DOI: 10.1007/s11837-017-2518-0

[67] Piga L, Pochetti F, Stoppa L. Recovering metals from red mud generated during alumina production. JOM. 1993;**45**(11):54-59. DOI: 10.1007/BF03222490

[68] Li G, Liu M, Rao M, et al. Stepwise extraction of valuable components from red mud based on reductive roasting with sodium salts. Journal of Hazardous Materials. 2014;**280**:774-780. DOI: 10.1016/j.jhazmat.2014.09.005

[69] Trushko VL, Utkov VA, Sivushov AA. Reducing the environmental impact of blast furnaces by means of red mud from alumina production. Steel in Translation. 2017;**47**(8):576-578. DOI: 10.3103/S0967091217080149